

Interface-Thickness Optimization of Lead-Free Oxide Multilayer Capacitors for High-Performance Energy Storage

Zixiong Sun,^{1,2†} Linxi Wang,^{1,2†} Ming Liu,^{1,2*} Chunrui Ma,² Zhongshuai Liang,^{1,2} Qiaolan Fan,^{1,2} Lu Lu,^{1,2} Xiaojie Lou,³ Hong Wang,^{1,2} Chun-Lin Jia^{1,2,4}

¹ School of Microelectronics, Xi'an Jiaotong University, Xi'an 710049, China

² State Key Laboratory for Mechanical Behavior of Materials, Xi'an Jiaotong University, Xi'an 710049, P. R. China

³ Frontier Institute of Science and Technology, Xi'an Jiaotong University, Xi'an 710049, China

⁴ Ernst Ruska Centre for Microscopy and Spectroscopy with Electrons, Forschungszentrum Jülich, D-52425 Jülich, Germany

† These authors contributed equally to this work.

* Electronic address: m.liu@xjtu.edu.cn

RESULTS AND DISCUSSION

Fig. S2 (a) shows the sketches of the multilayer films of $\text{Ba}_{0.7}\text{Ca}_{0.3}\text{TiO}_3$ (BCT) and $\text{BaZr}_{0.2}\text{Ti}_{0.8}\text{O}_3$ (BZT) with single period thickness $PT=0.25 H$ and total multilayer film thickness $MT=0.25 H, 0.5 H, 1 H, 1.5 H$ and $2 H$, where $H=100 \text{ nm}$. In comparison with those shown in Fig. 1 an extra sample film with $MT=1.5 H$ is added. Fig. S2 (b) is the typical x-ray diffraction (XRD) θ - 2θ scans for these multilayer films. All the BCT//BZT multilayers grown on Nb doped SrTiO_3 (NSTO) substrates are c -axis orientation with the interface relationships of $(001)_{\text{BCT}}// (001)_{\text{BZT}}// (001)_{\text{NSTO}}$ and $[100]_{\text{BCT}}// [100]_{\text{BZT}}// [100]_{\text{NSTO}}$. The BCT and BZT peaks are observed in the $MT=0.25 H$ bilayer film, while the satellite peaks, which are characteristics of a superlattices structure, can be clearly identified in all the others multilayer films, suggesting the $(00l)$ -oriented superlattices structures are successfully grown on NSTO substrates. Low-magnification high-angle annular dark field (HAADF) image with the corresponding selected area electron diffraction pattern (SAED) (in the inset) of the multilayer with $MT=2 H$ is displayed in Fig. S2 (c). The BCT (light area) and BZT (dark area) layers with clear interfaces in the multilayer system can be seen. In order to further reveal the interfacial strain states of all the multilayer films, the reciprocal space mapping around the (001) and the (103) planes have been carried out. The reciprocal space maps (RSMs) are illustrated in Fig. S2 (d) and (e). Corresponding lattice parameters of the in-plane (a/b) and out-of-plane (c) of all the multilayer films are calculated from the RSMs and are listed in Table S1. It can be concluded from the lattice parameters that there is almost no change in the stress state between substrates and multilayers except for the $0.25 H$ multilayer.

To systematically show the comprehensive energy storage performances of the BCT/BZT multilayer films with different PT and different MT at room temperature, the three-dimensional diagrams of E_B , P_{max} , ESD and η depend on periodic number and single

layer thickness are illustrated in Fig. S3. The maximum value of E_B and ESD with the value of 4.73 MV/cm and 52.4 J/cm³ is located at the multilayer film with PT= 0.125 H and MT=1 H, while the highest η of 81.2 % is obtained for the multilayer film with PT=0.25 and MT=2 H.

Fig. S4 is the illustration of the measuring procedure and distribution of interface charges. This illustration is to show the distribution of interface charges between the BCT and BZT layer vividly and also the effects to the electrical trees of those interface charges. When a certain electrical field is applied to the multilayer, the interface charges will give an inhibition to this spread, with increasing the electrical field.

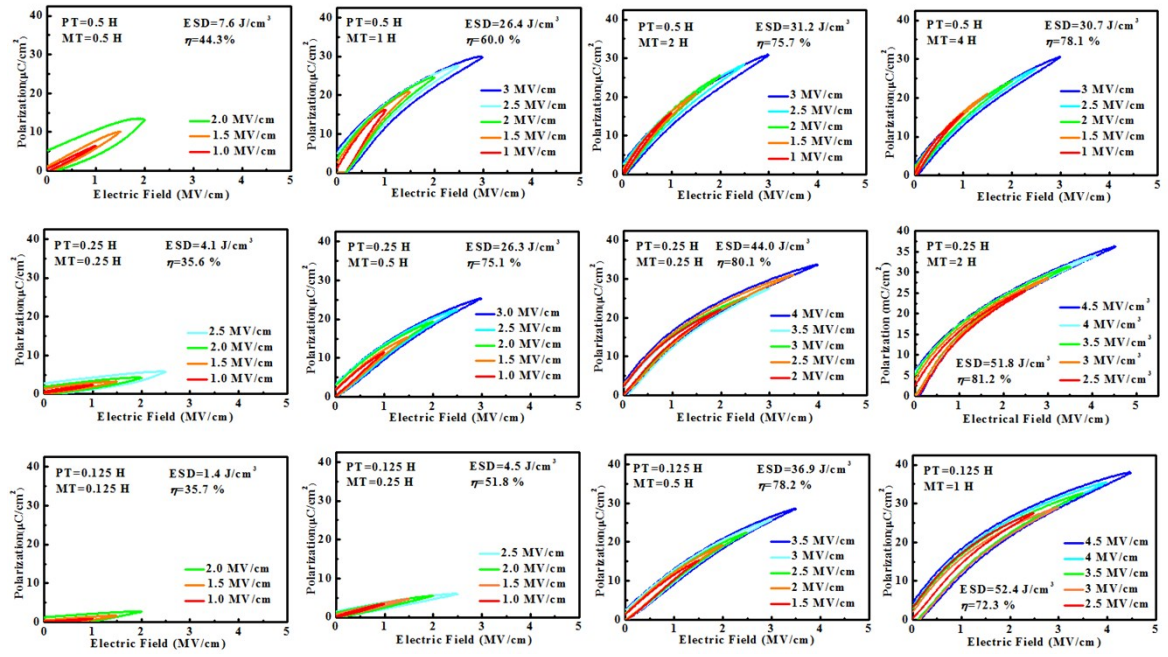


Figure. S1 The ferroelectric hysteresis loops for all the BCT/BZT multilayer films with PT from 0.125 H to 0.5 H and with different total thickness, grown on NSTO substrates. The display sequence of the data is arranged in correspondence with that of the multilayer films shown in Fig. 1.

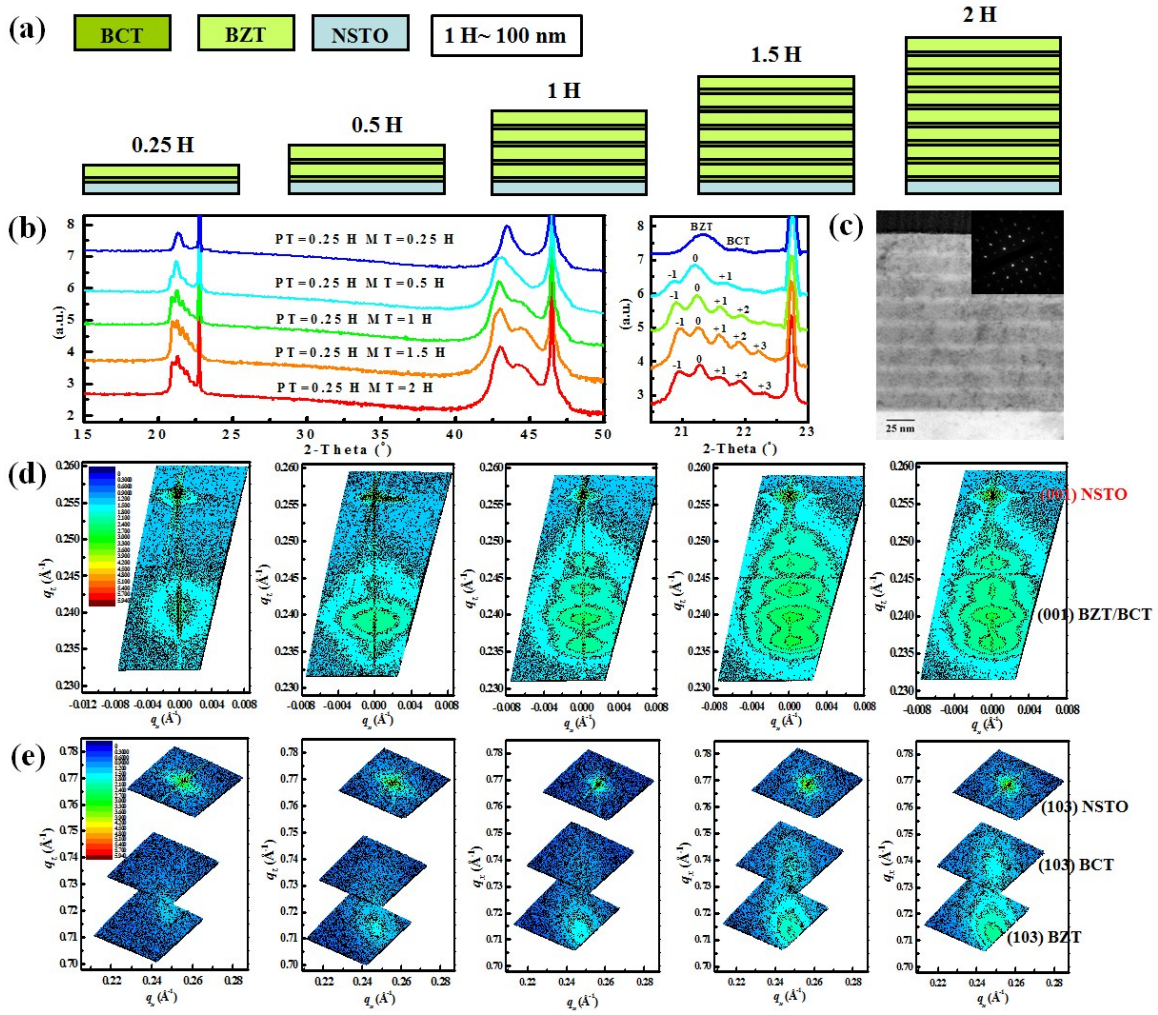


Figure. S2 (a) Sketch for the BCT/BZT multilayer films with periodic layer thickness $PT=0.25$ H and total thickness from 0.25 H to 2 H, grown on NSTO substrates. (b) Typical θ - 2θ scanning patterns for the BCT/BZT multilayer films with $PT=0.25$ H grown on NSTO substrates. Only (00 l) reflection peaks of the multilayers and the substrates are observed, indicating that all the multilayers are c -axis oriented. The enlarged θ - 2θ scans near the (001) peak are shown in the right part. For all the multilayer films, satellite peaks for superlattice periodicities can be clearly seen. (c) HAADF images and EDP patterns of the multilayer film with the thickness $MT=2$ H. (d) Reciprocal space maps taken around the (001) reflection of the BCT/BZT multilayer films with $PT=0.25$ H grown on NSTO substrates. (e) Reciprocal space maps taken around the (103) reflection of the BCT/BZT multilayer films with $PT=0.25$ H grown on NSTO substrates.

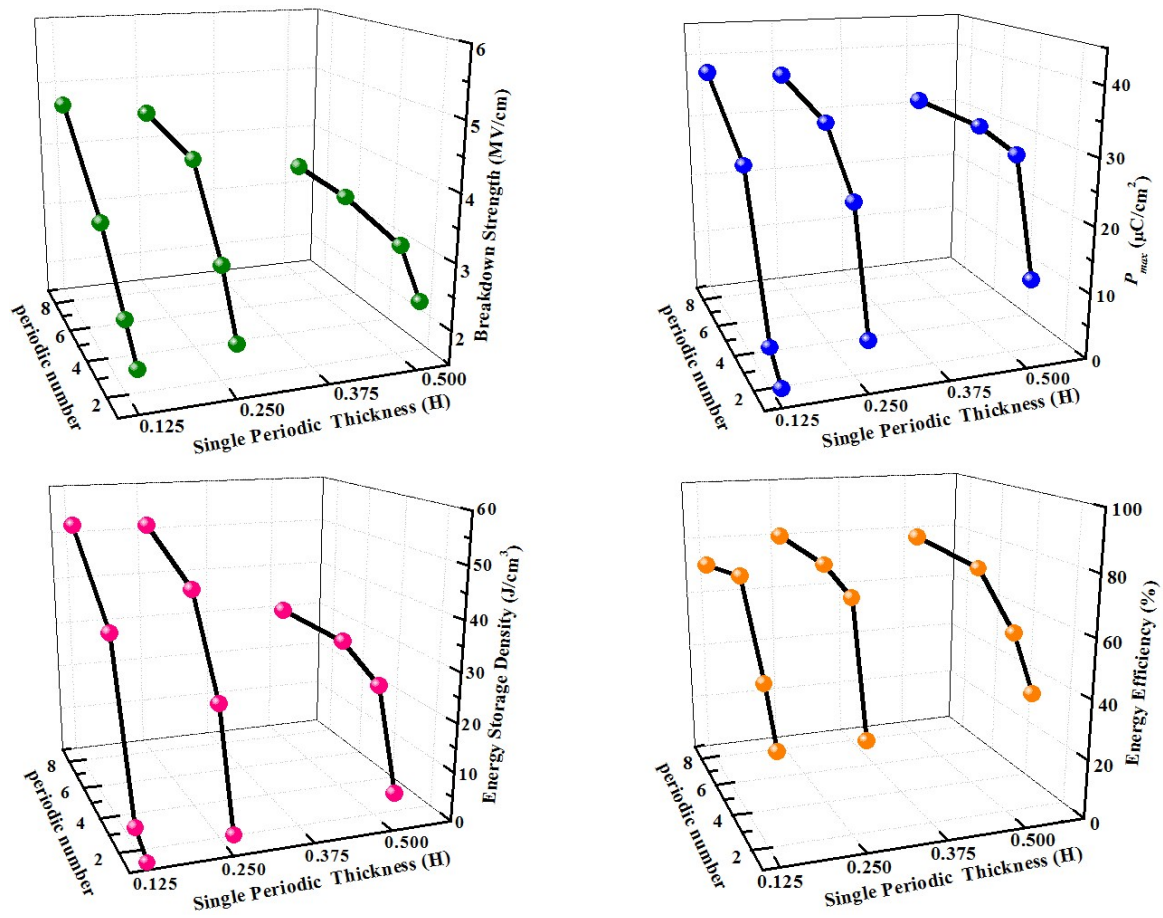


Figure. S3 Three-dimensional diagrams of E_B , P_{max} , ESD and η depend on periodic layer thickness PT and total thickness MT for all the BCT/BZT multilayer films grown on NSTO substrates.

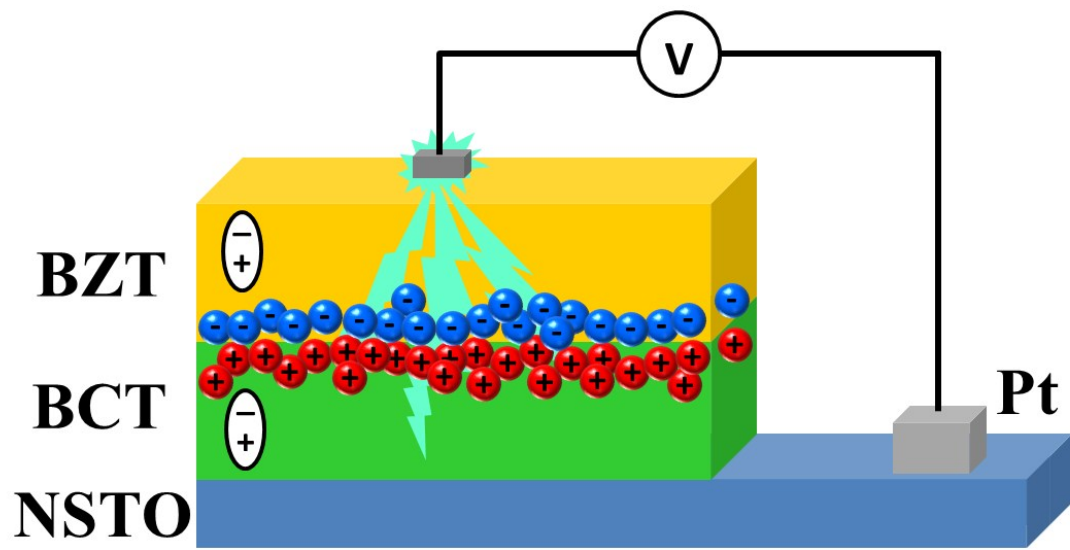


Figure. S4 Illustration of the measuring procedure and distribution of interface charges.

Table. S1 Thickness dependent lattice parameters of the BCT/BZT multilayers with N=4.

	Thickness	0.25 H	0.5 H	1 H	1.5 H	2 H
BZT	a (Å)	4.027	4.053	4.042	4.035	4.026
	c (Å)	4.165	4.203	4.206	4.206	4.209
BCT	a (Å)	-	-	4.038	4.027	4.022
	c (Å)	-	-	4.078	4.071	4.066